

Low-frequency ocean ambient noise on the Chukchi Shelf in the changing Arctic^{a)}

Julien Bonnel,^{1,b)} G. Bazile Kinda,² and Daniel P. Zitterbart¹

¹Applied Ocean Physics and Engineering, Woods Hole Oceanographic Institution, Woods Hole, Massachusetts 02540, USA

²Sciences et Techniques Marines, Service Hydrographique et Océanographique de la Marine, 13 rue du Chatellier, CS 92803, Brest 29228, France

ABSTRACT:

This article presents the study of a passive acoustic dataset recorded on the Chukchi Shelf from October 2016 to July 2017 during the Canada Basin Acoustic Propagation Experiment (CANAPE). The study focuses on the low-frequency (250–350 Hz) ambient noise (after individual transient signals are removed) and its environmental drivers. A specificity of the experimental area is the Beaufort Duct, a persistent warm layer intrusion of variable extent created by climate change, which favors long-range acoustic propagation. The Chukchi Shelf ambient noise shows traditional polar features: it is quieter and wind force influence is reduced when the sea is ice-covered. However, the study reveals two other striking features. First, if the experimental area is covered with ice, the ambient noise drops by up to 10 dB/Hz when the Beaufort Duct disappears. Further, a large part of the noise variability is driven by distant cryogenic events, hundreds of kilometers away from the acoustic receivers. This was quantified using correlations between the CANAPE acoustic data and distant ice-drift magnitude data (National Snow and Ice Data Center).

© 2021 Author(s). All article content, except where otherwise noted, is licensed under a Creative Commons Attribution (CC BY) license (<http://creativecommons.org/licenses/by/4.0/>). <https://doi.org/10.1121/10.0005135>

(Received 4 January 2021; revised 5 May 2021; accepted 11 May 2021; published online 9 June 2021)

[Editor: Hanne Sagen]

Pages: 4061–4072

I. INTRODUCTION

The Arctic Ocean has been undergoing massive climate warming induced changes over recent decades. The most prominent one is the decrease in sea ice coverage, thickness, and duration. Sea ice-free summers could appear as early as mid-century (Notz and SIMIP Community, 2020). In the Canada Basin, the ice-free area has increased by as much as 70% compared to the climatological mean (Wood *et al.*, 2015), making it one of the most impacted regions in the Arctic considering sea ice reduction and ocean stratification (McLaughlin *et al.*, 2011). Aside from reduced sea ice, the Beaufort Duct, a recurring Pacific warm water intrusion first observed in the early 1970s, has increased its geographic spread (Toole *et al.*, 2010). It has become persistent and more prominent throughout the year, as observed by the Woods Hole Oceanographic Institution's Ice-Tethered Profiler (ITP) program (Woods Hole Oceanographic Institution, 2016; Krishfield *et al.*, 2008; Toole *et al.*, 2011). Today, the Beaufort Duct (Duda, 2017) is present year-round in Arctic Ocean waters (Fig. 1) and extends at least up to 76° N (Krishfield *et al.*, 2008). Due to the significant impacts of the Beaufort Duct on the acoustic propagation, it has recently received increased attention in the literature (Ballard and Sagers, 2020; Chen *et al.*, 2019; Lynch *et al.*, 2018; Ozanich *et al.*, 2017).

Underwater ambient sound (ISO 18405:2017, 2017) is composed of the superposition of countless abiotic, biotic, and anthropogenic sounds. The main abiotic sound sources include sea surface processes, such as waves, precipitation, and wind stress, as well as geophysical processes, such as earthquakes and volcanic activities (Dziak *et al.*, 2011). In polar regions, the underwater ambient sound is heavily influenced by ice generated sounds, which are comprised of iceberg and sea ice melting (Glowacki *et al.*, 2018; Urick, 1971), ice cracking (Milne and Ganton, 1964), iceberg calving (Matsumoto *et al.*, 2014), iceberg vibrations (Müller *et al.*, 2005), and shearing and rubbing between moving ice blocks (Kinda *et al.*, 2015). Sea ice cover generally lowers the ambient noise by reducing the wind stress on the sea surface, limiting the creation of waves and bubbles. Marine mammals are another main component of the polar ocean underwater ambient sound (Ahonen *et al.*, 2017; Filun *et al.*, 2020; Haver *et al.*, 2017; Heimrich *et al.*, 2020; Menze *et al.*, 2017; Stafford *et al.*, 2007a). The polar oceans are generally quieter compared to other oceans due to fewer anthropogenic noise sources, such as shipping, construction, and geophysical prospection. Nonetheless, in the last 30 years, ship traffic in the Arctic has at least doubled (Judson, 2010) and thereby increased the anthropogenic footprint on the ambient sound. The expected further reduction of sea ice, opening up the North West Passage (the shortest route connecting Europe and Asia by sea) possibly for year-round shipping (Melia *et al.*, 2016) is likely to further increase ambient noise levels (ANLs) in the Arctic Ocean, especially on the Chukchi Shelf, where all North

^{a)}This paper is part of a special issue on Ocean Acoustics in the Changing Arctic.

^{b)}Electronic mail: jbonnel@whoi.edu, ORCID: 0000-0001-5142-3159.

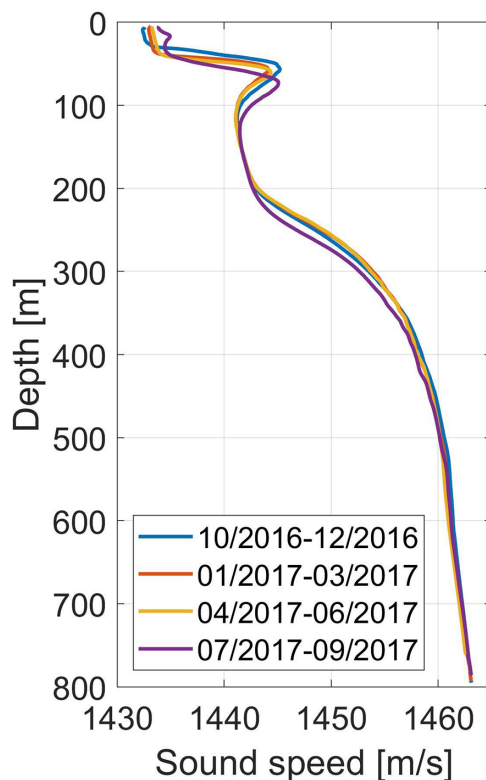


FIG. 1. (Color online) Chukchi Sea sound speed profiles: 741 ITP measurements within 300 km of the recording location have been used to build 3-month averages, showing the year-round existence of the Beaufort Duct in deep water.

West Passage traffic would sail through. Ship traffic in the Arctic has been shown to affect the behavior of Antarctic cod (Ivanova *et al.*, 2020). Also, half the sub-populations of Arctic marine mammals are susceptible to the impacts of increased shipping (Hauser *et al.*, 2018).

This study focuses on the Chukchi Shelf area. As stated in the Introduction, an important oceanographic feature is the Beaufort Duct. In conjunction with the disappearance of multi-year sea ice with deep underwater ridges, the duct is known to significantly improve the acoustic propagation conditions (Ballard and Sagers, 2020), which is favorable for underwater acoustic communication (Freitag *et al.*, 2015). In this paper, we study the impact of the Beaufort Duct on the low-frequency (250–350 Hz) ambient noise (obtained after removing transient signals from the ambient sound) on the Chukchi Shelf measured at the depth of the duct, using passive acoustic monitoring data from the Canada Basin Acoustic Propagation Experiment (CANAPE) (Worcester *et al.*, 2018). The considered low-frequency context is important for marine life (e.g., Menze *et al.*, 2017; Stafford *et al.*, 2007a) and is known to be impacted by human activities (Hildebrand, 2009). Geophysical noise, including cryogenic events, is another important source of noise in this frequency band (e.g., Kinda *et al.*, 2013; Urick, 1971). The frequency band considered in this study (250–350 Hz) is relatively narrow but is assumed to be representative of the low-frequency context. Last but not least,

this specific frequency band was occupied by several acoustic sources deployed during the CANAPE experiment (Ballard and Sagers, 2020; Worcester *et al.*, 2018). Consequently, the result of the present passive acoustic study can be compared with active acoustic studies from the CANAPE group.

The paper's main contributions are twofold. First, we find that underwater ANLs are increased by 5–10 dB/Hz when the Beaufort Duct is present on the Chukchi Shelf. Further, we demonstrate that during the Arctic winter, a pervasive ambient noise driver is distant cryogenic activity, hundreds of kilometers away from the recording location.

II. MATERIALS AND METHODS

A. The Canada Basin acoustic propagation experiment

The CANAPE was conducted in 2016 and 2017 in the Canada Basin (deep water, hereinafter DW-CANAPE) and on the Chukchi Shelf (shallow water, hereinafter SW-CANAPE). Many acoustic assets, both receivers and sources, were deployed as part of the experiment. This paper relies on a year-long passive acoustic dataset collected by Woods Hole Oceanographic Institution (WHOI) on the Chukchi Shelf (SW-CANAPE). Five “several hydrophone recording unit” (SHRU) moorings were deployed on the shelf edge. Each mooring consists of a vertical line hydrophone array (four channels) with temperature and pressure sensors.

Although the study focuses on the acoustic data collected by the SHRUs, the proposed method also relies on information collected using various DW-CANAPE and SW-CANAPE assets. In particular, our study benefits from the presence of seven physical oceanography moorings deployed by the University of Delaware on the Chukchi Shelf. Water temperature information, as shown in Fig. 5 of Ballard *et al.* (2020), was used to evaluate the presence of the Beaufort Duct on the SW-CANAPE area. Further, the study focuses on a frequency band that is occupied by a set of six acoustic sources deployed by the Scripps Institution of Oceanography in the DW-CANAPE area. Those signals are known to propagate from the deep Canada Basin to the shallow Chukchi Shelf (Ballard *et al.*, 2020). They constitute a nuisance for our study, and dedicated processing will be used to reject them.

B. Data

1. Acoustic data

This study uses passive acoustic data collected on a mooring called SHRUS, located at 72.908° N, 157.484° W, where the water depth is 445 m. This specific SHRU has been chosen as it was the mooring with the lowest self-noise. The four SHRUS hydrophones were placed at depths from 163 to 170.5 m with a regular sensor spacing of 2.5 m. Here, only the deepest hydrophone is used. The study also

considers data collected on a mooring called SHRU1, located at 72.907° N, 159.018° W, with water depth equal to 302 m. SHRU1 also has four hydrophones, but a single channel at depth 163 m is used. All the acoustic data were recorded continuously from October 22, 2016 to July 30, 2017, with sampling frequency $f_s = 3906.2$ Hz.

Most of the study focuses on the SHRU5 data. The data from SHRU1 will exclusively be used to assess the consistency of distant cryogenic noise drivers, and SHRU1 has been chosen to maximize the distance with SHRU5. SHRU1 and SHRU5 are separated by about 50 km.

2. Environmental data

This study involves a quantitative comparison of the acoustic data with various independent environmental data: local ice concentration (IC), local wind speed (WS), and global ice drift in the Arctic. Those are known to highly impact the low-frequency ambient sound ([Kinda et al., 2013](#)).

IC data are available online from the Integrated Climate Data Center ([ICDC, 2020](#)). The data have a daily period and a resolution of 12.5 km × 12.5 km. IC is given as the percentage of the area covered with sea ice for a given grid cell. It is obtained by satellite remote sensing (special sensor microwave/imager and special sensor microwave/imager sounder), and the ARTIST Sea Ice algorithm ([Kaleschke et al., 2001; Spreen et al., 2008](#)). Note that ICDC also applies a 5-day median filter to reduce the weather influence ([Kern et al., 2010](#)). In this article, we consider exclusively IC at the acoustic receiver locations.

WS data are available online from the European Centre for Medium-Range Weather Forecasts (ERA5 dataset) ([ECMWF, 2019](#)). The data have a time resolution of 3 h and a spatial resolution of 0.25° × 0.25°. WS (in m/s) are obtained by a combination of models and data assimilation to “reanalyze” archived observations. Here, again, our study focuses on local data at the receiver location.

Global ice drift over the Arctic is available online from the National Snow and Ice Data Center ([Tschudi et al., 2019](#)). The data are a daily two-dimensional (2D) vector field (in cm/s), with a spatial resolution of 25 km × 25 km. The data are obtained by satellite remote sensing (passive microwave or scatterometer) and a multi-sensor merging algorithm. In this article, the whole Arctic dataset is used. However, the 2D vector field is reduced to the one-dimensional (1D) ice-drift magnitude (IDM) at each grid point.

C. Data processing

1. Time segmentation

Based on local oceanographic observations, notably the ice cover and the potential presence of the Beaufort Duct, the measurement period is divided into three segments. To define the time segments, the potential presence of ice is defined using the IC. If IC is <15%, the sea is assumed to be ice-free. If IC is >85%, the sea is assumed to be ice-

covered. Further, the period with ice (IC >85%) is arbitrarily cut into two equal parts. The Beaufort Duct is assumed to be mostly present on the experimental area during the first period, and the validity of this assumption is discussed below.

The acoustic recording starts on October 22, 2016 and ends on July 30, 2017. Over this period, the time segmentation, based on IC, is as follows:

- October 22, 2016 to November 8, 2016: the sea is ice-free (IC <15%);
- November 23, 2016 to June 22, 2017: the sea is covered with ice (IC >85%);
- July 12, 2017 to July 30, 2017: the sea is ice-free (IC <15%).

During the periods that are not mentioned above (November 8–23, 2016 and June 22–July 12, 2017), the IC has intermediate values: the ice is either forming or retracting.

Further, the middle of the ice-covered period is March 8, 2017. In this study, this date is used as a proxy to mark the local disappearance of the Beaufort Duct. This choice is consistent with published oceanographic data showing that the Beaufort Duct gradually disappears from the CANAPE experimental area in March 2017 [[Ballard et al. \(2020\)](#), Fig. 5].

2. Spectral analysis of acoustic data

The acoustic data analysis relies on the assumption that the ambient sound can be described as the superposition of a diffuse broadband ambient noise and various individual transient signals. The acoustic data analysis is performed in the spectral domain. First, power spectral densities (PSD) (in dB re 1 $\mu\text{Pa}^2/\text{Hz}$) are computed to characterize the overall ambient sound. Further, ANLs (in dB re 1 $\mu\text{Pa}^2/\text{Hz}$) are computed to characterize the underlying diffuse noise ([Carey and Evans, 2011](#)). Note that ANL has been used in previous polar underwater acoustic studies ([Kinda et al., 2013; Roth et al., 2012](#)). It can be estimated by manually removing data snapshots with transient signals ([Roth et al., 2012](#)). Here, we use an automated algorithm, as proposed by ([Kinda et al., 2013](#)). The whole method is briefly described below.

Formally, the acoustic data are divided into 7 min snapshots, without overlap. For each snapshot, a short-time Fourier transform (STFT) is computed with a sliding window of 62.5 ms and 50% overlap. The resulting spectra (i.e., square modulus of the FT) are averaged to obtain an estimation of the PSD. This method is called Bartlett's method, or averaged periodogram ([Bartlett, 1948](#)). The PSD time series is representative of the long-term ambient noise ([Curtis et al., 1999](#)); it is now usually called a long-term spectral average (LTSA) (in dB re 1 $\mu\text{Pa}^2/\text{Hz}$).

The ANL is estimated using a process that relies on the same 7-min snapshots and on the same short-time spectra. However, instead of averaging the spectra, the ANL is estimated from the 15th percentile computed in each frequency

bin, following a statistical method presented in (Huillery *et al.*, 2008). This process is iterated on all snapshots, which leads to an ANL measure every 7 min.

The ANL time series is processed in two different manners. First, monthly histograms are computed to produce empirical probability of the power spectral densities (EPSD) (in dB re 1 $\mu\text{Pa}^2/\text{Hz}$) (Merchant *et al.*, 2013) of the ambient noise. Further, the 7-min ANL data are averaged into a frequency band to obtain a mean value in that band. Here, the chosen band is 250–350 Hz, and the corresponding mean ANL, centered around 300 Hz, is denoted ANL₃₀₀; it is assumed to be representative of the low-frequency ambient noise. This choice is similar to the one done by Kinda *et al.* (2013), who integrated ANL in 10–500 Hz. Note that the PSD time series is processed in the same way, leading to a mean PSD₃₀₀ in the 250–350 Hz band.

The central frequency chosen here (300 Hz) ensures that, on each mooring, the receivers are approximately spaced by $\lambda/2$, with λ the wavelength. Although no beamforming is considered in the current study, this choice opens the door to beamforming for future studies. Also, the short window that is used to compute STFT (62.5 ms) implied a relatively poor frequency resolution (~ 15 Hz). However, it is sufficient to analyze the 250–350 Hz band, and it allows good rejection of short transient signals (less than a few minutes) when computing the ANL. It notably allows us to filter the active source signals from DW-CANAPE.

3. Link between acoustic and environmental data

Correlation between ANL₃₀₀ and environmental data are computed to estimate the main noise drivers. The various datasets have different sampling periods: 7 min (ANL₃₀₀), 3 h (WS), and 24 h (IDM and IC). To compute correlation with a given environmental variable, ANL₃₀₀ is first decimated to the relevant sampling frequency (same as the environmental variable).

Correlations are computed between ANL₃₀₀ and the local environmental variable (IC and WS) at different time scales. The correlation between ANL₃₀₀ and IC is computed for the whole dataset, while the correlation between ANL₃₀₀ and WS is computed over 31-day sliding windows, without overlap.

Correlation between ANL₃₀₀ and IDM is computed for an area that covers the whole Arctic ocean (north of the ice-edge), as in Kinda *et al.* (2013). To do so, the ANL₃₀₀ is correlated with the IDM time series, as obtained at each pixel of the IDM map. Mathematically, for a given 2-month period centered on time t_0 , one computes the correlation map

$$M(x, y, t_0) = \Gamma[n(t_0), d(x, y, t_0)], \quad (1)$$

with x the latitude, y the longitude, Γ the Pearson correlation function, $n(t_0)$ the 2-month ANL₃₀₀ time series centered on t_0 , and $d(x, y, t_0)$ the 2-month time series centered on t_0 of the IDM at position (x, y) . The variable t_0 is incremented by

2-week amounts, effectively creating a 2-month sliding window with 75% of overlap.

All correlation results are quantified using the correlation coefficient R and the p value. Correlation coefficients reported in this paper all have $p < 0.05$. Correlation coefficients with $p > 0.05$ are deemed to be statistically insignificant and are not reported here. The local correlations (with WS and IC) are obtained using ANL₃₀₀ from SHRU5. The spatial correlations (with IDM) are obtained using data from SHRU5 and SHRU1.

Last but not least, ANL₃₀₀ histograms are computed for the three time periods defined in Sec. II C 1.

III. RESULTS

A. Ambient noise levels and influence of ice cover

The PSD-LTSA, ANL-LTSA, PSD₃₀₀, and ANL₃₀₀ are shown in Fig. 2, along with the IC. The ANLs are clearly lower than the PSDs. A detailed examination of the LTSA confirms that transient signals present in the PSD-LTSA are absent in the ANL-LTSA. This is notably true for the active source signals from the DW-CANAPE experiment, which have been filtered. This phenomenon is more evident from PSD₃₀₀ and ANL₃₀₀: the PSD₃₀₀ dispersion (i.e., the apparent thickness of the blue curve) is due to the acoustic sources. A zoom over a few days of data (October 27–29) confirms that SPL₃₀₀ contains recurrent large spikes, i.e., the active source signals.

Both ANL and PSD qualitatively show that the ambient sound is quieter when the sea is covered with ice. This is quantitatively confirmed by the correlation between ANL and IC. The correlation coefficient $R = -0.6$ clearly indicates that ANL increases when IC decreases, and vice versa.

Monthly EPSD are presented in Fig. 3, with mean IC indicated in red in each subplot. The EPSD confirm the ANL trend. November 2016 corresponds to an intermediate situation with a mean IC of 53%. December 2016 to June 2017 are months during which the sea is fully ice-covered (mean IC >90%). They all have ANLs that are significantly lower than July 2017, a period when the sea is mostly ice-free (mean IC = 25%). During the ice-covered period, the ANLs have a decreasing pattern that starts in March 2016. While very low ANLs occur in March, they are more frequent from April to June. The noise floor of the recording system is reached by a limited number of data points in March/April for frequencies above 200 Hz and levels below 35 dB re 1 mPa²/Hz.

The time variability of the ambient noise is made more concise by plotting ANP₃₀₀ histograms during the three time periods defined in Sec. II C 1. The result, illustrated in Fig. 4, shows three distributions that are clearly distinct. ANP₃₀₀ is clearly highest when the sea is ice-free, with a mean value $MV = 87.4$ dB/Hz and a most probable value $MP = 88.5$ dB/Hz. Further, when the sea is covered with ice, ANP₃₀₀ is larger when the duct is present ($MV = 78.2$ dB/Hz, $MP = 76$ dB/Hz) than when the duct is absent ($MV = 73.1$ dB/Hz, $MP = 67.5$ dB/Hz).

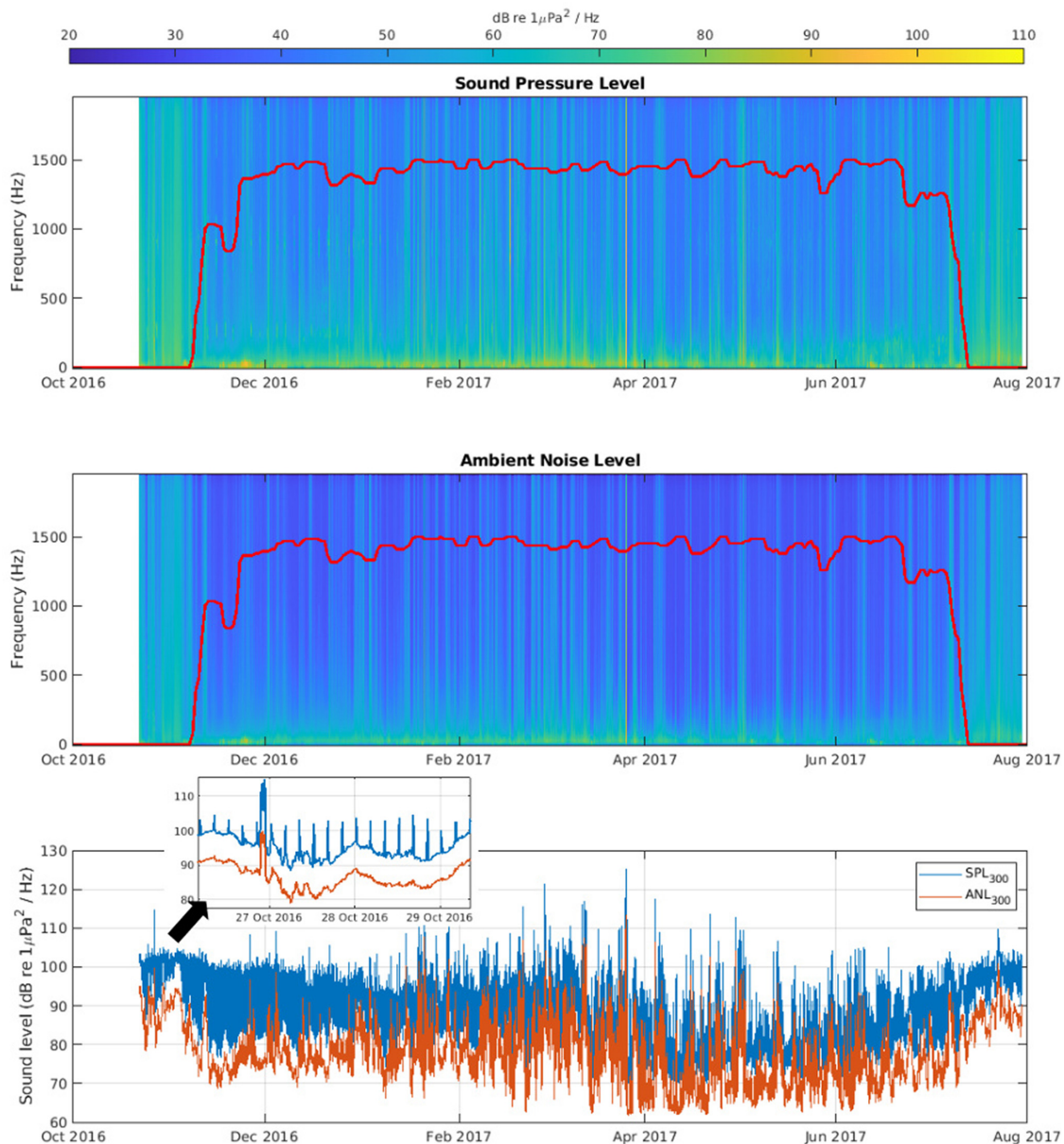


FIG. 2. (Color online) Long-term spectral averages for the raw data (top) and for the estimated ambient noise (middle) and associated mean values in the frequency band 250–350 Hz (bottom). In the top two panels, the red curve is proportional to the local IC, with a minimal value of 0% and a maximal value of 100%.

B. Influence of local WS

Monthly scatter plots showing the link between ANL_{300} and WS are presented in Fig. 5. A significant correlation between ANL_{300} and WS is found every month. Correlation coefficients are higher during months that are not fully ice-covered (November 2016 and July 2017), with $R \sim 0.7$. When the experimental area is fully ice-covered, correlation coefficients are lower but significant ($0.2 < R < 0.6$), even when the Beaufort Duct is present (early December 2016 to end of February 2017). The relationship between ANL_{300} and WS also depends on the ice condition: a WS change creates a larger ANL_{300} change when the sea is not covered with ice (see the slope of the black lines in Fig. 5).

The scatter plots also reproduce the result from Fig. 4: when the sea is covered with ice, the ANL_{300} values are much lower when the duct is absent than when it is present.

C. Influence of distant ice drift

An example of spatial correlation between ANL_{300} and IDM is presented in Fig. 6, both for SHRU1 and SHRU5. The maps (left column) show a clear correlation with distant drift magnitude, with a similar pattern for the two receivers. The figure also shows (right column) the ANL_{300} time series, along with the ID time series at the location where the correlation is maximum (red cross on the maps). This shows that the correlation is driven by overall tendencies,

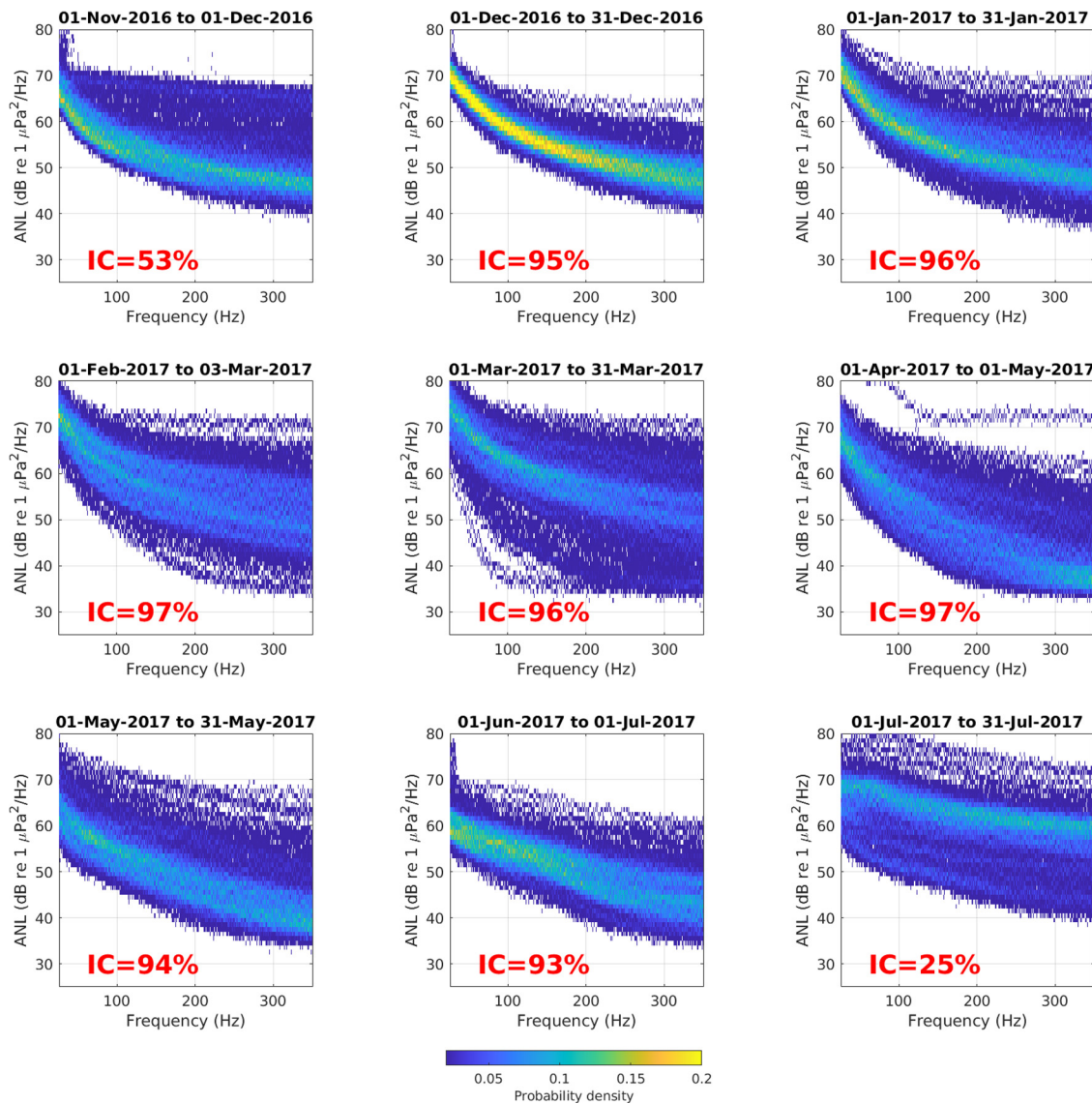


FIG. 3. (Color online) Monthly EPSD of ANLs and monthly averages of the local IC.

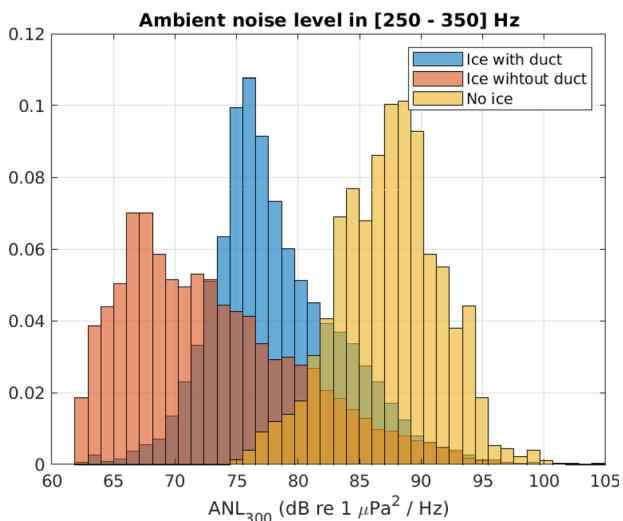


FIG. 4. (Color online) Histograms of the averaged ANLs (250–350 Hz) depending on the ice and duct conditions.

not just by strong transient events. This is further confirmed by the high R values (SHRU5: $R \sim 0.6$; SHRU1: $R \sim 0.7$).

Although Fig. 6 is an illustrative example, it has features that are representative of other time periods. Spatial correlations were computed from November 1, 2016 to July 30, 2017. The time period with significant results is from December 1, 2016 to May 30, 2017, with $0.4 < R < 0.7$. At other times (November 2016, June and July 2016), the ID data are too scarce (i.e., with a lot of missing points) for the correlation to be meaningful.

All the correlation maps for SHRU5 are presented in Fig. 7. Over this whole period, the position of the correlation maximum stays between latitudes 75° N and 77° N, while its longitude is gradually moving eastward from 180° W to 150° W. The distance between this point and the acoustic receivers is between 270 and 770 km. Last but not least, an animated figure that shows all the results (correlation maps and time series) for SHRU1 and SHRU5 is provided as supplementary material.² When comparing the results between

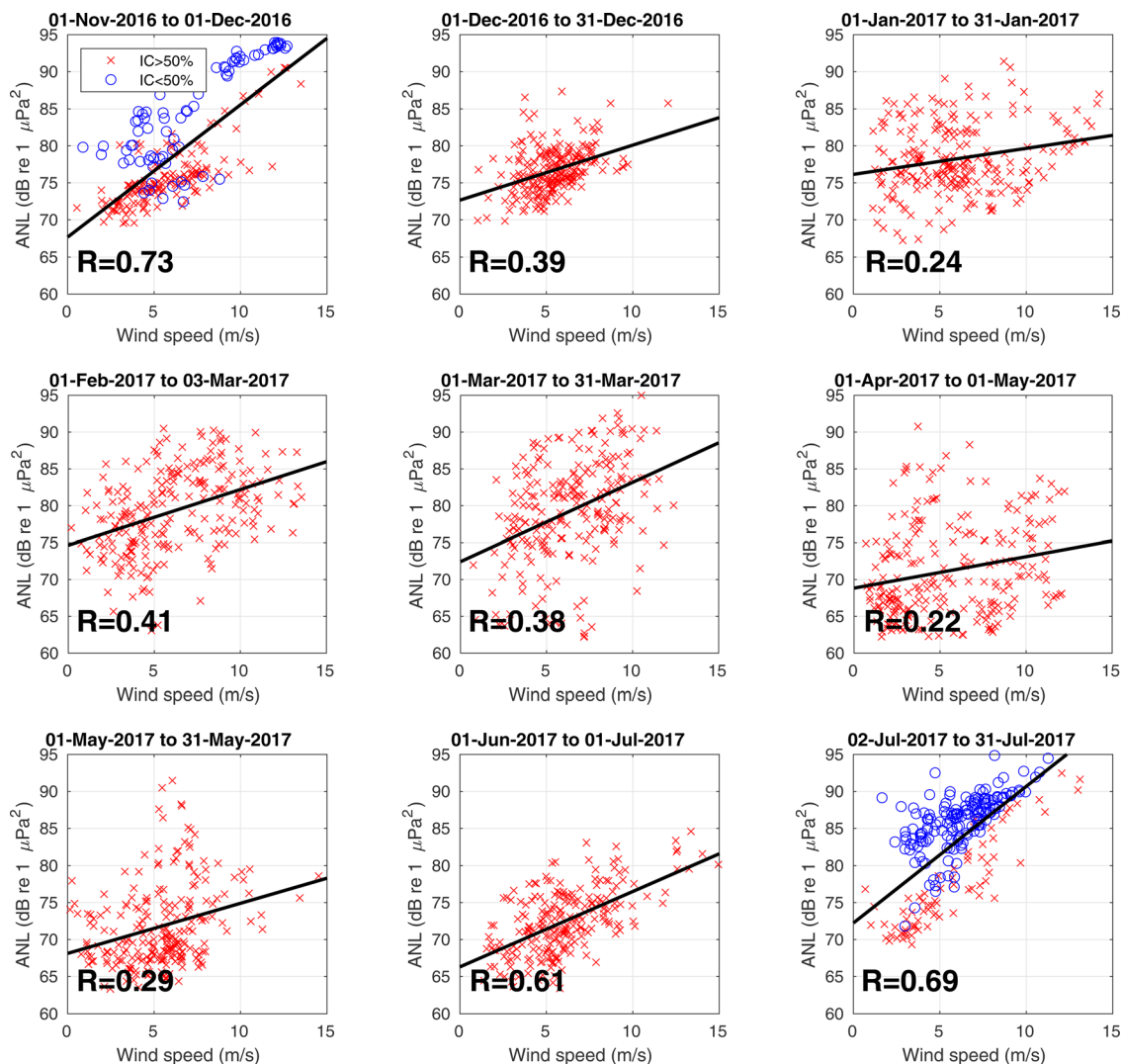


FIG. 5. (Color online) Three-hour averaged ANLs in 250–350 Hz versus WS and associated linear fit and correlation coefficient (R). All the p values are <0.001 . The data points are segmented into two groups, depending on the local IC value: blue circles represent data with $IC < 50\%$ while red crosses represent data with $IC > 50\%$.

the two acoustic datasets, the IDM grid point that maximizes the correlation is the same for SHRU1 and SHRU5 four times out of nine. A detailed examination of all the correlation maps shows that when the grid point is not strictly the same, the overall correlation area is nonetheless identical.

IV. DISCUSSION

This study demonstrates that the low-frequency (250–350 Hz) ambient noise on the Chukchi Shelf is driven by local (WS, IC), distant (IDM), and pervasive (Beaufort Duct) oceanographic features. As in many polar areas, the ambient noise largely depends on the local ice cover; it shows a classic quiet-under-ice pattern (Dziak *et al.*, 2015; Kinda *et al.*, 2013; Menze *et al.*, 2017). Further, ambient noise is also driven by local WS: it tends to increase when WS increases. Although our dataset covers a very short period (about 3 weeks) with open-sea conditions, it still shows that the relationship between ambient noise and WS

differs based on ice condition, the impact of WS being smaller when the area is fully covered with ice. This is a well-known polar phenomenon that can be found both in the Arctic (e.g., Roth *et al.*, 2012) and in the Antarctic (e.g., Menze *et al.*, 2017). More specifically, the highest correlation between WS and noise is in November 2016. This corresponds to a period of transition during which the local IC is highly variable, the experimental area consisting of a mixture of water and ice. Studies in the marginal ice zone showed that such environments are characterized by high levels of low-frequency noise. Such noise is indirectly generated by wind, which creates interactions between ice floes and waves or swells (Diachok and Winokur, 1974; Johannessen *et al.*, 2003).

More interestingly, our study is one of the few that link long-term ambient noise to distant cryogenic activity. As in Kinda *et al.* (2013), we demonstrate that ambient noise is correlated with IDM events that occur hundreds of kilometers away from the acoustic measurement (up to 770 km).

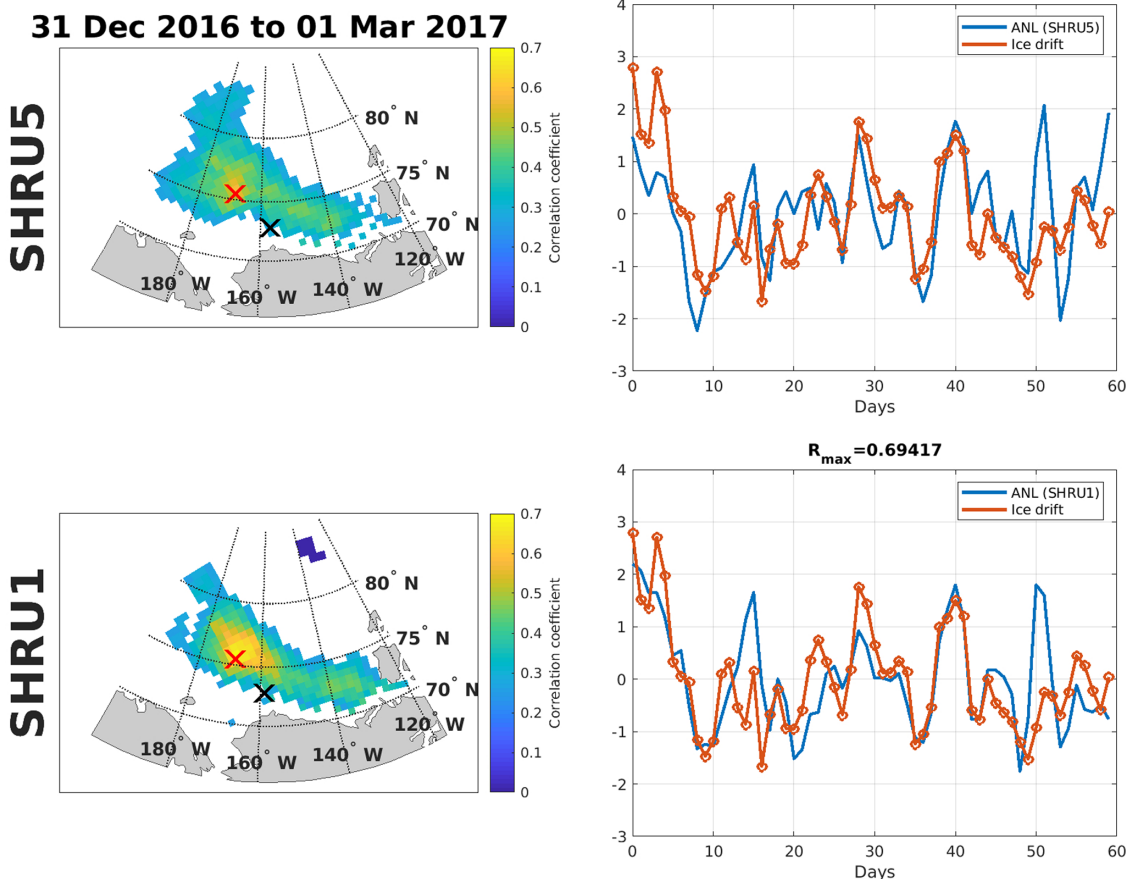


FIG. 6. (Color online) Spatial correlation between ANL (250–350 Hz) and ice drift for SHRU5 and SHRU1. The maps (left) show the spatial correlation between the ANL and the ice drift, for SHRU5 (top) and SHRU1 (bottom). On each map, the black cross is the position of the acoustic receiver, while the red cross is the position where the correlation is maximum. The color scale gives the value of the correlation coefficient R when $p < 0.05$, while white color indicates locations with $p \geq 0.05$. The time series (right) shows the normalized ambient noise data (averaged over 2 days) and the normalized ice-drift evolution at the location where the correlation is maximum (i.e., the position that is highlighted by a red cross on the corresponding map).

Further, we demonstrate for the first time how, over the 6 months of the Arctic winter, the location of an important cryogenic noise driver drifts by more than 900 km. This analysis has been performed on two datasets that were collected on moorings separated by ~ 50 km. Both datasets show very similar results. We thus hypothesize that the cryogenic sound source that is observed here radiates noise over most of the Alaskan Chukchi Shelf.

Additionally, our result is the first to demonstrate the profound impact of the Beaufort Duct on the ambient sound. If the experimental area is ice-covered, the low-frequency ambient noise drops by 5–10 dB/Hz when the Beaufort Duct disappears. This confirms that a significant part of the ambient noise is driven by distant sound sources. Interestingly, some of the ambient noise variability remains driven by distant cryogenic events, even when the duct is absent from the experimental area (March to May), and thus the environment is less favorable for long distance propagation. This is likely because the experimental area is still covered with ice, which tends to cover the local surface noise drivers. As a result, ANLs are low, but some of the variability of the remaining noise is still driven by distant sources. Although this study focuses on IDM, other sources likely contribute to

the low-frequency noise, including diverse cryogenic phenomena (Collins *et al.*, 2019) and marine mammals (Stafford *et al.*, 2007b).

The importance of the Beaufort Duct to long-range acoustic propagation is not a new topic. It has been predicted by acoustic propagation models, e.g., see Fig. 5 from Lynch *et al.* (2018), which shows propagation within the Beaufort Duct at 250 Hz. It has also been numerically and experimentally investigated during the CANAPE experiment. Low-frequency signals (200–300 Hz) from sources located in the Canada Basin were recorded at our experimental sites, with propagation distance between 370 and 520 km (Ballard *et al.*, 2020). Over the course of the experiment (1 year), the active source received levels (either modeled or numerically measured) differ by up to 60 dB, reaching their lowest levels from March to July (Ballard *et al.*, 2020). This temporal variability, driven by the disappearance of the Beaufort Duct on the Chukchi Shelf in March and by ice melt in early July, is similar to what we observe in the ANL data. However, the observed variability is much slower for the ANL (up to 10 dB) than for the active source signals (up to 60 dB). Indeed, a direct comparison between the dB levels cannot be done, since one is a specific

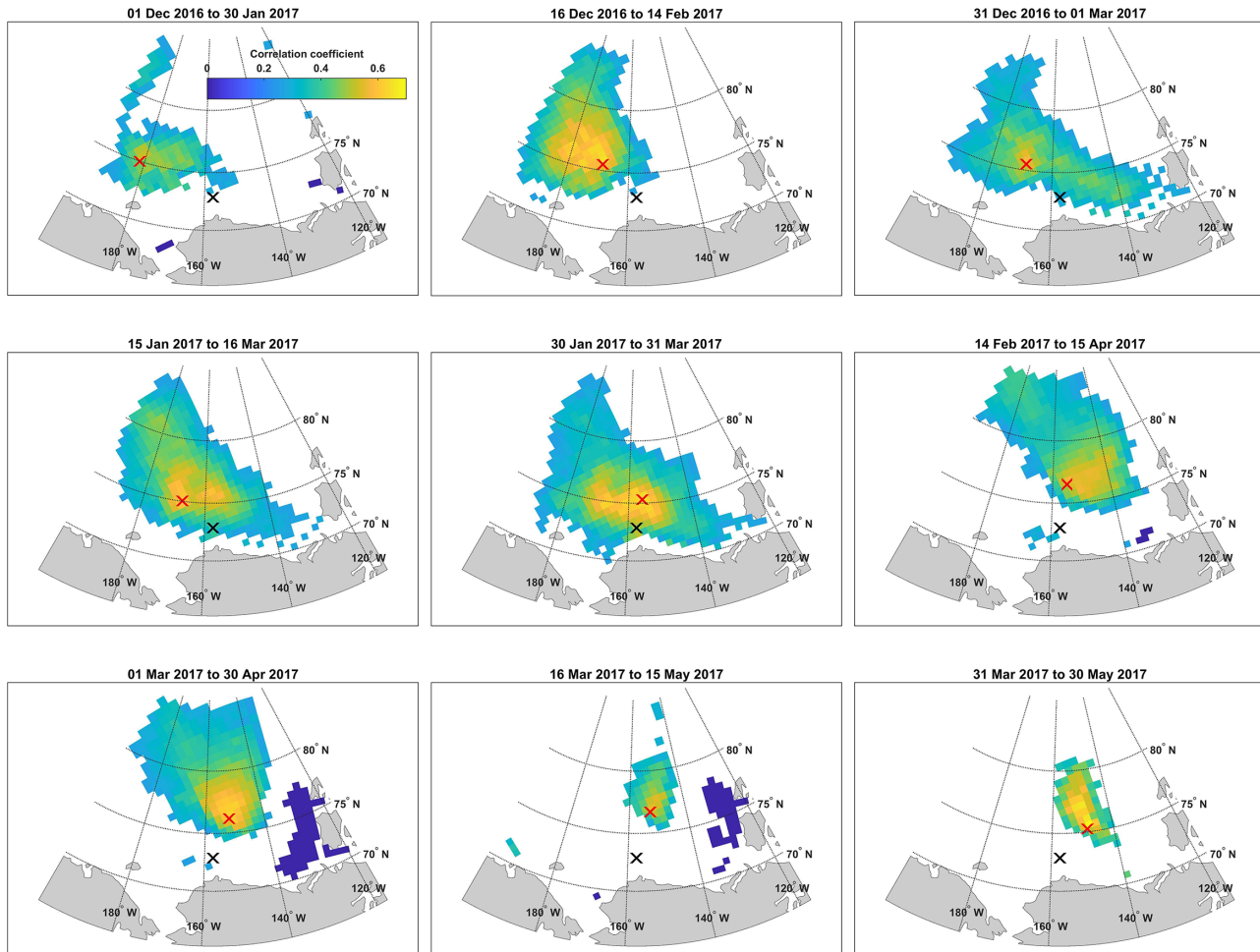


FIG. 7. (Color online) Correlation maps between the mean ANL (250–350 Hz) and the IDM (SHRU5). On each map, the black cross is the position of the acoustic receiver, while the red cross is the position where the correlation is maximum. The color scale gives the value of the correlation coefficient R when $p < 0.05$, while white color indicates locations with $p \geq 0.05$.

point-to-point propagation scenario (active acoustics) while the other integrates a spatial continuum of natural sources (passive acoustics). Still, our result shows that the oceanographic conditions that drive long-range acoustic propagation are also important to understand the ambient sound.

Importantly, one must consider that in our study, the importance of the Beaufort Duct is likely magnified by the depth of our acoustic recorders. Deployment depth has specifically been chosen to be within the duct to maximize the listening range. If a similar study was done using a recorder at another depth (e.g., bottom moored), the impact of the Beaufort Duct likely would be smaller.

Nonetheless, the persistence and increasing geographic spread of the Beaufort Duct has large implications for the ocean ambient noise in the Chukchi Shelf and Beaufort Sea. Underwater acoustic communication (Freitag *et al.*, 2015) becomes possible over larger distances or with less power, opening new perspectives of communication with and navigation of long-range under-ice autonomous vehicles (Kaminski *et al.*, 2010; Kukulya *et al.*, 2016). Under-ice acoustic float networks that utilize sound sources for float localization can operate over longer distances, and acoustic

tomography experiments can be conducted with less acoustic power while keeping the same footprint. Further, the ambient noise variability due to the changing environmental conditions needs to be properly accounted for in ambient noise models. Those are needed to assess the acoustic footprint of anthropogenic activities as well as to evaluate the performance of sonar systems.

The changing Beaufort ambient sound not only has impacts on technical applications; it also affects the ecosystem. As an important example, the Beaufort Duct could increase the communication space of bowhead whales. Bowhead whales have a large call repertoire (Clark and Johnson, 1984), ranging from ~ 100 to ~ 3000 Hz. They notably produce frequency modulated calls with most of the energy below 500 Hz, and they dive to duct-relevant depths (Heide-Jørgensen *et al.*, 2013; Simon *et al.*, 2009). Bowhead calls have been detected and localized over dozens of kilometers (Bonnel *et al.*, 2014). Their active acoustic space is estimated to range up to 130 km for low-frequency calls (~ 100 Hz) and up to 40 km for higher frequencies (Tervo *et al.*, 2012), which is significantly lower than for fin and blue whales. A larger active acoustic space, created by

favorable propagation conditions in the Beaufort Duct, could be beneficial for communication within the Bering–Chukchi–Beaufort stock or eventually facilitate an acoustic link across different bowhead stocks.

Despite opportunities that arise due to an increase in communication range, improved acoustic propagation naturally increases the overall ocean ANL as shown in this study. This needs to be considered in light of the changing Arctic. The improved acoustic propagation conditions will amplify the effects of the expected increased vessel traffic (Halliday *et al.*, 2017), hydrocarbon exploration, and associated construction efforts along the Chukchi Shelf (Gering and Zaki, 2020), posing significant risk to a marine life that still is naive to anthropogenic noise.

The impact of underwater noise on marine life has been intensively studied in the last decades (Erbe *et al.*, 2019). Endemic to the Arctic Ocean, bowhead whales have been shown to react to airgun sounds by changing their calling rates (Blackwell *et al.*, 2015), which is triggered depending on the sound exposure level. The use of airguns for hydrocarbon exploration or shipping under increased underwater acoustic propagation conditions would insonify larger areas, thus likely changing the behavior of more animals at the same time, which might be detrimental to the population (Halliday *et al.*, 2020). Such effects need to be carefully considered and might trigger a re-evaluation of current protection measures, such as mitigation radii.

The same argument can be made for any Arctic marine species that has shown significant behavioral responses to anthropogenic noise. Arctic cod, for example, has been shown to change its movements and behavior in response to shipping noise potentially scaring it off its feeding grounds (Ivanova *et al.*, 2020). Our understanding of behavioral impacts of underwater noise on invertebrates is still in its infancy (Jolivet *et al.*, 2016; Tidau and Briffa, 2016), and nothing is known of the potential impact of noise on Arctic invertebrates (PAME, 2019).

Overall, our results have profound implications for noise forecasting in a rapidly changing Arctic. They demonstrate the importance of global propagation to correctly understand the acoustical environment. This, more than ever, will be of paramount importance to forecast—and mitigate—the impact of anthropogenic activities on the Arctic acoustical environment.

ACKNOWLEDGMENTS

This research was supported by the Independent Research and Development Program at WHOI and by the Office of Naval Research (ONR) under Grant Nos. N00014-19-1-2627 and N00014-18-1-2811. J.B. warmly acknowledges D. Cazau (ENSTA Bretagne, France) for helpful discussion and code sharing. The acoustic data collection effort was supported by the ONR under Grant No. N00014-15-1-2196 (Principal Investigator: Y.-T. Lin, WHOI). Thanks also go to crew members of the R/V Sikuliaq and USCGC Healy for assisting in mooring

operations. The ITP data were collected and made available by WHOI.

²See supplementary material at <https://www.scitation.org/doi/suppl/10.1121/10.0005135> for the time evolution of the spatial correlation between ambient noise level (ANL₃₀₀) and IDM.

- Ahonen, H., Stafford, K. M., de Steur, L., Lydersen, C., Wiig, Ø., and Kovacs, K. M. (2017). “The underwater soundscape in western Fram Strait: Breeding ground of Spitsbergen’s endangered bowhead whales,” *Mar. Pollut. Bull.* **123**(1), 97–112.
- Ballard, M. S., Badiey, M., Sagers, J. D., Colosi, J. A., Turgut, A., Pecknold, S., Lin, Y.-T., Proshutinsky, A., Krishfield, R., Worcester, P. F., and Dzieciuch, M. A. (2020). “Temporal and spatial dependence of a yearlong record of sound propagation from the Canada Basin to the Chukchi Shelf,” *J. Acoust. Soc. Am.* **148**(3), 1663–1680.
- Ballard, M. S., and Sagers, J. D. (2020). “A yearlong record of ambient sound on the Chukchi Shelf,” *J. Acoust. Soc. Am.* **148**(4), 2482–2482.
- Bartlett, M. (1948). “Smoothing periodograms from time-series with continuous spectra,” *Nature* **161**(4096), 686–687.
- Blackwell, S. B., Nations, C. S., McDonald, T. L., Thode, A. M., Mathias, D., Kim, K. H., Greene, C. R., Jr., and Macrander, A. M. (2015). “Effects of airgun sounds on bowhead whale calling rates: Evidence for two behavioral thresholds,” *PLoS One* **10**(6), e0125720.
- Bonnel, J., Thode, A., Blackwell, S., Kim, K., and Macrander, A. (2014). “Range estimation of bowhead whale (*Balaena mysticetus*) calls in the Arctic using a single hydrophone,” *J. Acoust. Soc. Am.* **136**(1), 145–155.
- Carey, W. M., and Evans, R. B. (2011). *Ocean Ambient Noise: Measurement and Theory* (Springer, New York).
- Chen, R., Poulsen, A., and Schmidt, H. (2019). “Spectral, spatial, and temporal characteristics of underwater ambient noise in the Beaufort Sea in 1994 and 2016,” *J. Acoust. Soc. Am.* **145**(2), 605–614.
- Clark, C. W., and Johnson, J. H. (1984). “The sounds of the bowhead whale, *Balaena mysticetus*, during the spring migrations of 1979 and 1980,” *Can. J. Zool.* **62**(7), 1436–1441.
- Collins, M. D., Turgut, A., Menis, R., and Schindall, J. A. (2019). “Acoustic recordings and modeling under seasonally varying sea ice,” *Sci. Rep.* **9**(1), 1–11.
- Curtis, K. R., Howe, B. M., and Mercer, J. A. (1999). “Low-frequency ambient sound in the North Pacific: Long time series observations,” *J. Acoust. Soc. Am.* **106**(6), 3189–3200.
- Diachok, O. I., and Winokur, R. S. (1974). “Spatial variability of underwater ambient noise at the Arctic ice-water boundary,” *J. Acoust. Soc. Am.* **55**(4), 750–753.
- Duda, T. F. (2017). “Acoustic signal and noise changes in the Beaufort Sea Pacific Water duct under anticipated future acidification of Arctic Ocean waters,” *J. Acoust. Soc. Am.* **142**(4), 1926–1933.
- Dziak, R. P., Bohnenstiel, D. R., Stafford, K. M., Matsumoto, H., Park, M., Lee, W. S., Fowler, M. J., Lau, T.-K., Hazel, J. H., and Mellinger, D. K. (2015). “Sources and levels of ambient ocean sound near the Antarctic Peninsula,” *PLoS One* **10**(4), e0123425.
- Dziak, R. P., Hammond, S. R., and Fox, C. G. (2011). “A 20-year hydroacoustic time series of seismic and volcanic events in the Northeast Pacific Ocean,” *Oceanography* **24**(3), 280–293.
- ECMWF (2019). “ERA5,” <https://ecmwf.int/en/forecasts/datasets/reanalysis-datasets/era5> (Last viewed May 27, 2021).
- Erbe, C., Marley, S. A., Schoeman, R. P., Smith, J. N., Trigg, L. E., and Embeling, C. B. (2019). “The effects of ship noise on marine mammals—A review,” *Front. Mar. Sci.* **6**, 606.
- Filun, D., Thomisch, K., Boebel, O., Brey, T., Širović, A., Spiesecke, S., and Van Opzeeland, I. (2020). “Frozen verses: Antarctic minke whales (*Balaenoptera bonaerensis*) call predominantly during austral winter,” *R. Soc. Open Sci.* **7**(10), 192112.
- Freitag, L., Ball, K., Partan, J., Koski, P., and Singh, S. (2015). “Long range acoustic communications and navigation in the Arctic,” in Proceedings of OCEANS 2015—MTS/IEEE, October 19–22, Washington, DC, pp. 1–5.
- Gering, S., and Zaki, M. (2020). “Academic analysis on the feasibility of shipping liquefied natural gas from Alaska’s North Slope,” Technical Report (University of Alaska’s Arctic Domain Awareness Center, Anchorage, AK).

- Glowacki, O., Deane, G. B., and Moskalik, M. (2018). "The intensity, directionality, and statistics of underwater noise from melting icebergs," *Geophys. Res. Lett.* **45**(9), 4105–4113 <https://doi.org/10.1029/2018GL077632>.
- Halliday, W. D., Insley, S. J., Hilliard, R. C., de Jong, T., and Pine, M. K. (2017). "Potential impacts of shipping noise on marine mammals in the western Canadian Arctic," *Mar. Pollut. Bull.* **123**(1), 73–82.
- Halliday, W. D., Pine, M. K., Citta, J. J., Harwood, L., Hauser, D. D., Hilliard, R. C., Lea, E. V., Loseto, L. L., Quakenbush, L., and Insley, S. J. (2020). "Potential exposure of beluga and bowhead whales to underwater noise from ship traffic in the Beaufort and Chukchi Seas," *Ocean Coastal Manage.* **204**, 105473.
- Hauser, D. D., Laidre, K. L., and Stern, H. L. (2018). "Vulnerability of Arctic marine mammals to vessel traffic in the increasingly ice-free Northwest Passage and Northern Sea Route," *Proc. Natl. Acad. Sci. U.S.A.* **115**(29), 7617–7622.
- Haver, S. M., Klinck, H., Niekirk, S. L., Matsumoto, H., Dziak, R. P., and Miksis-Olds, J. L. (2017). "The not-so-silent world: Measuring Arctic, Equatorial, and Antarctic soundscapes in the Atlantic Ocean," *Deep Sea Res. Part I Oceanogr. Res. Pap.* **122**, 95–104.
- Heide-Jørgensen, M. P., Laidre, K. L., Nielsen, N. H., Hansen, R. G., and Røstad, A. (2013). "Winter and spring diving behavior of bowhead whales relative to prey," *Anim. Biotelemetry* **1**(1), 1–13.
- Heimrich, A. F., Halliday, W. D., Frouin-Mouy, H., Pine, M. K., Juanes, F., and Insley, S. J. (2020). "Vocalizations of bearded seals (*Ereignathus barbatus*) and their influence on the soundscape of the western Canadian Arctic," *Mar. Mamm. Sci.* **37**, 173–192.
- Hildebrand, J. A. (2009). "Anthropogenic and natural sources of ambient noise in the ocean," *Mar. Ecol. Prog. Ser.* **395**, 5–20.
- Huillery, J., Millioz, F., and Martin, N. (2008). "On the description of spectrogram probabilities with a chi-squared law," *IEEE Trans. Signal Process.* **56**(6), 2249–2258.
- ICDC (2020). "Sea-Ice concentration for Arctic & Antarctic (ASI-SSMI)," <https://icdc.cen.uni-hamburg.de/en/seaiceconcentration-asi-ssmi.html> (Last viewed May 27, 2021).
- ISO 18405:2017 (2017). "Underwater acoustics—Terminology" (International Organization for Standardization, Geneva, Switzerland).
- Ivanova, S. V., Kessel, S. T., Espinoza, M., McLean, M. F., O'Neill, C., Landry, J., Hussey, N. E., Williams, R., Vagle, S., and Fisk, A. T. (2020). "Shipping alters the movement and behavior of Arctic cod (*Boreogadus saida*), a key-stone fish in Arctic marine ecosystems," *Ecol. Appl.* **30**(3), e02050.
- Johannessen, O. M., Sagen, H., Sandven, S., and Stark, K. V. (2003). "Hotspots in ambient noise caused by ice-edge eddies in the Greenland and Barents Seas," *IEEE J. Ocean. Eng.* **28**(2), 212–228.
- Jolivet, A., Tremblay, R., Olivier, F., Gervaise, C., Sonier, R., Genard, B., and Chauvaud, L. (2016). "Validation of trophic and anthropic underwater noise as settlement trigger in blue mussels," *Sci. Rep.* **6**(1), 1–8.
- Judson, B. (2010). "Trends in Canadian Arctic shipping traffic—Myths and rumours," in Proceedings of the Twentieth International Offshore and Polar Engineering Conference, June 20–25, Beijing, China.
- Kaleschke, L., Lüpkes, C., Vihma, T., Haarpaintner, J., Bochert, A., Hartmann, J., and Heygster, G. (2001). "SSM/I sea ice remote sensing for mesoscale ocean-atmosphere interaction analysis," *Can. J. Remote Sens.* **27**(5), 526–537.
- Kaminski, C., Crees, T., Ferguson, J., Forrest, A., Williams, J., Hopkin, D., and Heard, G. (2010). "12 days under ice—An historic AUV deployment in the Canadian High Arctic," in *Proceedings of 2011 IEEE/OES Autonomous Underwater Vehicles*, September 1–3, Monterey, CA.
- Kern, S., Kaleschke, L., and Spreen, G. (2010). "Climatology of the Nordic (Irminger, Greenland, Barents, Kara and White/Pechora) Seas ice cover based on 85 GHz satellite microwave radiometry: 1992–2008," *Tellus A* **62**(4), 411–434.
- Kinda, B. G., Simard, Y., Gervaise, C., Mars, J. I., and Fortier, L. (2013). "Under-ice ambient noise in Eastern Beaufort Sea, Canadian Arctic, and its relation to environmental forcing," *J. Acoust. Soc. Am.* **134**(1), 77–87.
- Kinda, G. B., Simard, Y., Gervaise, C., Mars, J. I., and Fortier, L. (2015). "Arctic underwater noise transients from sea ice deformation: Characteristics, annual time series, and forcing in Beaufort Sea," *J. Acoust. Soc. Am.* **138**(4), 2034–2045.
- Krishfield, R., Toole, J., Proshutinsky, A., and Timmermans, M.-L. (2008). "Automated ice-tethered profilers for seawater observations under pack ice in all seasons," *J. Atmos. Ocean. Technol.* **25**(11), 2091–2105.
- Kukulya, A., Bellingham, J., Kaeli, J., Reddy, C., Godin, M., and Conmy, R. (2016). "Development of a propeller driven long range autonomous underwater vehicle (LRAUV) for under-ice mapping of oil spills and environmental hazards: An Arctic Domain Center of Awareness project (ADAC)," in *Proceedings of 2016 IEEE/OES Autonomous Underwater Vehicles (AUV)*, November 6–9, Tokyo, Japan, pp. 95–100.
- Lynch, J. F., Gawarkiewicz, G. G., Lin, Y.-T., Duda, T. F., and Newhall, A. E. (2018). "Impacts of ocean warming on acoustic propagation over continental shelf and slope regions," *Oceanography* **31**(2), 174–181.
- Matsumoto, H., Bohnenstiehl, D. R., Tournadre, J., Dziak, R. P., Haxel, J. H., Lau, T.-K., Fowler, M., and Salo, S. A. (2014). "Antarctic icebergs: A significant natural ocean sound source in the Southern Hemisphere," *Geochem. Geophys. Geosyst.* **15**(8), 3448–3458.
- McLaughlin, F., Carmack, E., Proshutinsky, A., Krishfield, R. A., Guay, C., Yamamoto-Kawai, M., Jackson, J. M., and Williams, B. (2011). "The rapid response of the Canada Basin to climate forcing: From bellwether to alarm bells," *Oceanography* **24**(3), 146–159.
- Melia, N., Haines, K., and Hawkins, E. (2016). "Sea ice decline and 21st century trans-Arctic shipping routes," *Geophys. Res. Lett.* **43**(18), 9720–9728 <https://doi.org/10.1002/2016GL069315>.
- Menze, S., Zitterbart, D. P., Van Opzeeland, I., and Boebel, O. (2017). "The influence of sea ice, wind speed and marine mammals on southern ocean ambient sound," *R. Soc. Open Sci.* **4**(1), 160370.
- Merchant, N. D., Barton, T. R., Thompson, P. M., Pirotta, E., Dakin, D. T., and Dorocic, J. (2013). "Spectral probability density as a tool for ambient noise analysis," *J. Acoust. Soc. Am.* **133**(4), EL262–EL267.
- Milne, A., and Ganton, J. (1964). "Ambient noise under Arctic-Sea ice," *J. Acoust. Soc. Am.* **36**(5), 855–863.
- Müller, C., Schindlein, V., Eckstaller, A., and Miller, H. (2005). "Singing icebergs," *Science* **310**(5752), 1299–1299.
- Notz, D., and SIMIP Community (2020). "Arctic sea ice in CMIP6," *Geophysical Res. Lett.* **47**(10), e2019GL086749.
- Ozanich, E., Gerstoft, P., Worcester, P. F., Dzieciuch, M. A., and Thode, A. (2017). "Eastern Arctic ambient noise on a drifting vertical array," *J. Acoust. Soc. Am.* **142**(4), 1997–2006.
- PAME (2019). "Underwater noise in the arctic: A state of knowledge report" (Protection of the Arctic Marine Environment (PAME) Secretariat, Akureyri, Iceland).
- Roth, E. H., Hildebrand, J. A., Wiggins, S. M., and Ross, D. (2012). "Underwater ambient noise on the Chukchi Sea continental slope from 2006–2009," *J. Acoust. Soc. Am.* **131**(1), 104–110.
- Simon, M., Johnson, M., Tyack, P., and Madsen, P. T. (2009). "Behaviour and kinematics of continuous ram filtration in bowhead whales (*Balaena mysticetus*)," *Proc. R. Soc. B Biol. Sci.* **276**(1674), 3819–3828.
- Spreen, G., Kaleschke, L., and Heygster, G. (2008). "Sea ice remote sensing using AMSR-E 89-GHz channels," *J. Geophys. Res.* **113**(C2), C02S03 <https://doi.org/10.1029/2005JC003384>.
- Stafford, K. M., Mellinger, D. K., Moore, S. E., and Fox, C. G. (2007b). "Seasonal variability and detection range modeling of baleen whale calls in the Gulf of Alaska, 1999–2002," *J. Acoust. Soc. Am.* **122**(6), 3378–3390.
- Stafford, K. M., Moore, S., Spillane, M., and Wiggins, S. (2007a). "Gray whale calls recorded near Barrow, Alaska, throughout the winter of 2003–04," *Arctic* **60**, 167–172, available at <https://www.jstor.org/stable/40513132>.
- Tervo, O. M., Christoffersen, M. F., Simon, M., Miller, L. A., Jensen, F. H., Parks, S. E., and Madsen, P. T. (2012). "High source levels and small active space of high-pitched song in bowhead whales (*Balaena mysticetus*)," *PLoS One* **7**(12), e52072.
- Tidau, S., and Briffa, M. (2016). "Review on behavioral impacts of aquatic noise on crustaceans," *Proc. Mtgs. Acoust.* **27**, 010028.
- Toole, J. M., Krishfield, R. A., Timmermans, M.-L., and Proshutinsky, A. (2011). "The ice-tethered profiler: Argo of the Arctic," *Oceanography* **24**(3), 126–135.
- Toole, J. M., Timmermans, M.-L., Perovich, D. K., Krishfield, R. A., Proshutinsky, A., and Richter-Menge, J. A. (2010). "Influences of the ocean surface mixed layer and thermohaline stratification on Arctic Sea ice in the central Canada Basin," *J. Geophys. Res.* **115**(C10), C10018 <https://doi.org/10.1029/2009JC005660>.
- Tschudi, M., Meier, W., Stewart, J., Fowler, C., and Maslanik, J. (2019). "Polar pathfinder daily 25 km EASE-grid sea ice motion vectors, version 4," <https://doi.org/10.5067/INAWUWO7QH7B> (Last viewed December 14, 2020).

- Urick, R. (1971). "The noise of melting icebergs," *J. Acoust. Soc. Am.* **50**(1B), 337–341.
- Wood, K. R., Bond, N. A., Danielson, S. L., Overland, J. E., Salo, S. A., Stabeno, P. J., and Whitefield, J. (2015). "A decade of environmental change in the Pacific Arctic region," *Prog. Oceanogr.* **136**, 12–31.
- Woods Hole Oceanographic Institution (2016). "Ice-tethered profiler," <https://whoi.edu/itp> (Last viewed December 17, 2020).
- Worcester, P. F., Dzieciuch, M. A., Colosi, J. A., Proshutinsky, A. Y., Krishfield, R. A., Nash, J. D., and Kemp, J. N. (2018). "The 2016–2017 deep-water Canada Basin Acoustic Propagation Experiment (CANAPE): An overview," *J. Acoust. Soc. Am.* **144**(3), 1665–1665.